

Measurement of the $\text{In}_{0.52}\text{Al}_{0.48}\text{As}$ valence-band hydrostatic deformation potential and the hydrostatic-pressure dependence of the $\text{In}_{0.52}\text{Al}_{0.48}\text{As}/\text{InP}$ valence-band offset

C. N. Yeh and L. E. McNeil

Department of Physics and Astronomy, University of North Carolina at Chapel Hill, Chapel Hill, North Carolina 27599-3255

R. E. Nahory and R. Bhat

Bellcore, Red Bank, New Jersey 07701-0740

(Received 1 May 1995)

We have measured the $\text{In}_{0.52}\text{Al}_{0.48}\text{As}$ valence-band hydrostatic deformation potential from the hydrostatic-pressure dependence of the $\text{In}_{0.52}\text{Al}_{0.48}\text{As}/\text{InP}$ valence-band offset which was measured from 0 to 35 kbar at room temperature. Due to the type-II band lineup, the radiative recombinations across the InP band gap and between the InP conduction band and the $\text{In}_{0.52}\text{Al}_{0.48}\text{As}$ valence band were both observed in the photoluminescence spectra. This enables us to measure directly the changes of the valence-band offset under pressure. The hydrostatic-pressure derivative of the valence-band offset was measured to be 0.0 ± 0.4 meV/kbar. The predictions of the pressure dependence from band-offset models (dielectric midgap and model-solid theories) agree with the measurement to within 1 meV/kbar. The $\text{In}_{0.52}\text{Al}_{0.48}\text{As}$ valence-band hydrostatic deformation potential is found to be -0.8 eV which compares well with the dielectric midgap theory. Using the reported pressure dependence of the GaAs/AlAs valence-band offset, the valence-band hydrostatic deformation potentials of $\text{In}_x\text{Al}_{1-x}\text{As}$ ($0 \leq x \leq 0.52$) are linearly interpolated as $-1.9x + 0.2$ eV.

I. INTRODUCTION

The $\text{In}_{0.52}\text{Al}_{0.48}\text{As}/\text{InP}$ heterostructure has received much attention recently because the high electron saturation velocity and mobility of the InP channel make it suitable for high-power electronic device applications.¹ Further improvement is possible by varying the alloy composition such that strain in $\text{In}_x\text{Al}_{1-x}\text{As}$ raises the conduction-band offset to increase the two-dimensional electron density. However, the intrinsic band offset of the $\text{In}_x\text{Al}_{1-x}\text{As}/\text{InP}$ heterostructure also changes with the alloy composition. In order to achieve an optimum design, it is necessary to accurately determine $\text{In}_x\text{Al}_{1-x}\text{As}$ strain-induced band-edge shifts, which are proportional to band-edge hydrostatic deformation potentials. Although the band-gap hydrostatic deformation potential can be accurately measured from the band-gap hydrostatic-pressure dependence by optical absorption or photoluminescence (PL) techniques, individual band-edge potentials are more difficult to measure because of the difficulty of finding a pressure-insensitive reference level. Indirect measurements of GaAs and InP conduction-band hydrostatic deformation potentials, obtained from analysis of the electron mobility, spread over a range as large as the band-gap values.^{2,3} Based on the experimental observation⁴ that energy separations of transition-metal defect levels are independent of host materials, it was proposed that transition-metal defect levels are fixed relative to the vacuum level and independent of bulk materials. Using transition-metal defects as reference levels, band-edge hydrostatic deformation potentials of GaAs and InP have been directly measured by deep-level transient spectroscopy.³ Since the band-edge shift induced by

hydrostatic pressure is proportional to the hydrostatic deformation potential, the band-edge hydrostatic deformation potential of a III-V compound lattice matched to GaAs or InP can be accurately measured using the hydrostatic-pressure dependence of the corresponding valence-band (conduction-band) offset and GaAs or InP band-edge hydrostatic deformation potentials. The measurement of $\text{In}_{0.52}\text{Al}_{0.48}\text{As}$ deformation potentials from the pressure dependence of the $\text{In}_{0.52}\text{Al}_{0.48}\text{As}/\text{InP}$ valence-band offset gives a more reliable value than does the fitting of the measured electron mobility to a theoretical model because alloy-disorder scattering is the dominant mechanism influencing the electron mobility at low temperature, rather than acoustic-phonon-deformation-potential scattering.^{5,6}

The lattice-matched $\text{In}_{0.52}\text{Al}_{0.48}\text{As}/\text{InP}$ heterostructure has a type-II band lineup, in which the conduction- and valence-band energy positions of $\text{In}_{0.52}\text{Al}_{0.48}\text{As}$ are both higher than those of InP (see the inset in Fig. 1). Three peaks were observed in low temperature PL studies.⁷⁻⁹ Two of them are related to transitions arising from the bulk semiconductors, and the lowest-energy peak near 1.2 eV is identified as the interface transition from the InP conduction band to the $\text{In}_{0.52}\text{Al}_{0.48}\text{As}$ valence band.¹⁰ This feature of the spectrum enables us to directly measure the hydrostatic-pressure dependence of the $\text{In}_{0.52}\text{Al}_{0.48}\text{As}/\text{InP}$ valence-band offset by monitoring the shifts of the InP and interface peaks under pressure. From the pressure dependence of the $\text{In}_{0.52}\text{Al}_{0.48}\text{As}/\text{InP}$ valence-band offset, we have measured the $\text{In}_{0.52}\text{Al}_{0.48}\text{As}$ valence-band hydrostatic deformation potential and compare it with the predictions from band offset models (dielectric midgap² and model-solid theories¹¹). Together

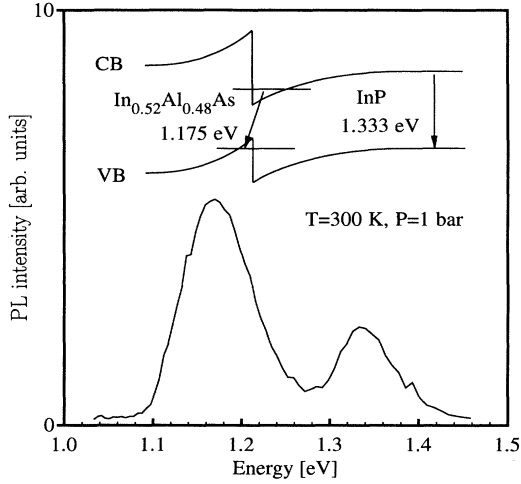


FIG. 1. PL spectrum at room temperature and atmospheric pressure. The inset shows the band diagram.

with the reported pressure dependence of the GaAs/AlAs valence-band offset,¹² the valence-band hydrostatic deformation potentials of $\text{In}_x\text{Al}_{1-x}\text{As}$ ($0 \leq x \leq 0.52$) are linearly interpolated from those of AlAs and $\text{In}_{0.52}\text{Al}_{0.48}\text{As}$.

II. EXPERIMENT

The sample consisted of a 500-Å InP buffer layer and 7500-Å $\text{In}_{0.52}\text{Al}_{0.48}\text{As}$ grown on the n^+ InP substrate by metalorganic chemical vapor deposition. The details of the growth have been described elsewhere.¹³ After thinning down to $\sim 100 \mu\text{m}$ from the InP substrate side, portions of the wafer were cleaved into $\sim 100 \times 100 \mu\text{m}^2$ chips for the pressure measurement. A Merrill-Basset diamond anvil cell with an Inconel gasket was used, with a pressure-transmitting medium of a 4:1 mixture of methanol and ethanol. The hydrostatic pressure was determined from ruby fluorescence using the λ^5 scale.¹⁴ The PL measurement was excited with the 488-nm line of an Ar-ion laser at 300 K. The laser beam was focused to a spot of about 1-mm diameter with an excitation power 0.3 W. The luminescence from the sample was dispersed and detected by a 0.22-m spectrometer and a liquid-nitrogen-cooled Ge detector using standard lock-in amplification techniques. The energy resolution was better than 6 meV. The ruby fluorescence was analyzed using a 0.85-m spectrometer and a photomultiplier.

III. RESULTS AND DISCUSSION

A. Pressure dependence of the valence-band offset

The PL spectrum at room temperature and pressure is shown in Fig. 1. The peaks at energies 1.175 and 1.333 eV are associated with the recombination across the interface and the InP band-to-band transition from the substrate. The band-to-band transition from $\text{In}_{0.52}\text{Al}_{0.48}\text{As}$

was not observed at room temperature (its band gap is 1.439 eV at room temperature¹⁵). The pressure-induced changes of the PL spectra and peak energies from 0 to 35 kbar are shown in Figs. 2 and 3. The hydrostatic-pressure derivative of the InP peak is linearly fitted as 8.0 ± 0.3 meV/kbar. The hydrostatic-pressure derivatives of n -type ($N_D = 5 \times 10^{15} \text{ cm}^{-3}$) and heavily doped ($N_D = 4 \times 10^{18} \text{ cm}^{-3}$) InP have been reported to be 8.4 (Ref. 16) and 7.9 meV/kbar (Ref. 17), respectively. This discrepancy is accounted for by the doping-dependent variations of the electron effective mass and the dielectric constant under pressure.¹⁷ Our value is consistent with that of heavily doped InP. This is also supported by the free-carrier concentration of $5 \times 10^{18} \text{ cm}^{-3}$, estimated from the full width at half maximum (73 meV) of the InP peak at atmospheric pressure.¹⁸ The interface peak follows the InP peak closely as the pressure is changed and its hydrostatic-pressure derivative is linearly fitted to be 7.9 ± 0.5 meV/kbar.

Although InP and $\text{In}_{0.52}\text{Al}_{0.48}\text{As}$ are closely lattice matched at atmospheric pressure, the elastic constants of the two are different and a lattice-mismatch strain will develop when they are compressed. This influence on the valence-band offset has to be taken into account in addition to the hydrostatic-pressure effect. Since the InP substrate is much thicker, the $\text{In}_{0.52}\text{Al}_{0.48}\text{As}$ layer will accommodate to the InP lattice and suffer a tetragonal distortion. The change of the lattice constant under hydrostatic pressure can be determined from the Murnaghan equation¹⁹

$$\frac{\Delta a}{a_0} = -\frac{1}{3} \left\{ 1 - \left[1 + \frac{B_1}{B_0} p \right]^{-1/B_1} \right\}, \quad (1)$$

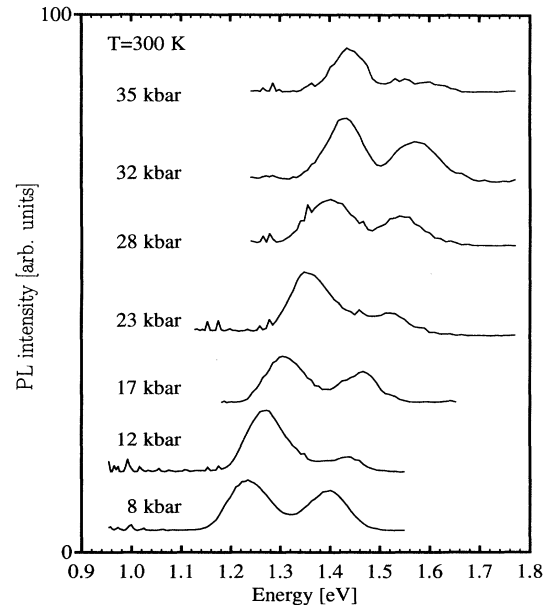


FIG. 2. Typical PL spectra under pressure.

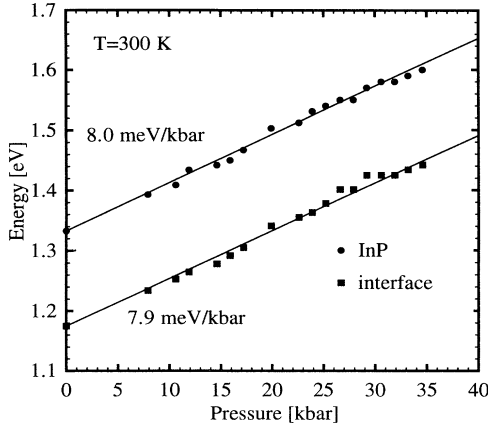


FIG. 3. PL peak energies vs pressure.

where a_0 , p , B_0 , and B_1 are the lattice constant at zero pressure, the hydrostatic pressure, the bulk modulus, and the first pressure derivative of the bulk modulus,²⁰ respectively. The material parameters for InP and $\text{In}_{0.52}\text{Al}_{0.48}\text{As}$ are listed in Table I. The in-plane strain of the $\text{In}_{0.52}\text{Al}_{0.48}\text{As}$ layer is given by

$$\varepsilon = \frac{a_p^{\text{InP}} - a_p^{\text{InAlAs}}}{a_p^{\text{InAlAs}}}, \quad (2)$$

where a_p denotes the lattice constant under pressure. ε is found to be smaller than 0.002 at 35 kbar. (Note that the lattice constant of $\text{In}_{0.52}\text{Al}_{0.48}\text{As}$ is changed by 1.5% as the pressure is increased from 0 to 35 kbar.) The strain-induced shift of the band gap (from the conduction to the heavy-hole band)^{11,21} is

$$\Delta E_{\text{strain}} = 2a_{\text{hy}} \left[1 - \frac{c_{12}}{c_{11}} \right] \varepsilon - b \left[1 + \frac{2c_{12}}{c_{11}} \right] \varepsilon, \quad (3)$$

where a_{hy} , b , and c_{ij} denote the band-gap hydrostatic deformation potential, the valence-band shear deformation potential, and the elastic constants, respectively. Using

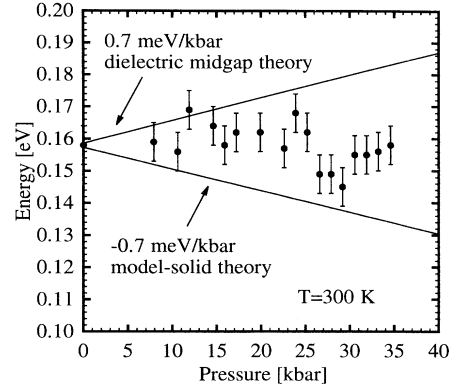


FIG. 4. Pressure dependence of the valence-band offset. The predictions from dielectric midgap and model-solid theories are shifted up to match the difference between the energies of the peaks in the PL spectrum at atmospheric pressure.

the parameters for $\text{In}_{0.52}\text{Al}_{0.48}\text{As}$ given in Table I, the pressure derivative of the strain-induced shifts ΔE_{strain} is estimated to be -0.2 meV/kbar. Since the hydrostatic-pressure derivative of the band gap of $\text{In}_{0.52}\text{Al}_{0.48}\text{As}$ has been reported as 10.1 meV/kbar,²² the influence of different lattice compression between InP and $\text{In}_{0.52}\text{Al}_{0.48}\text{As}$ is much less than the hydrostatic-pressure effect and can be ignored.

The valence-band offset can be obtained from (see Fig. 1)

$$\Delta E_{\text{VBO}} = E_g^{\text{InP}} - E^{\text{interface}} + E^{\text{confinement}}, \quad (4)$$

where E_g^{InP} , $E^{\text{interface}}$, and $E^{\text{confinement}}$ denote the InP band gap, the transition energy across the interface, and the total configuration energies of the electron and heavy hole. Because the difference of the band-gap hydrostatic-pressure derivatives between InP and $\text{In}_{0.52}\text{Al}_{0.48}\text{As}$ is 2.1 meV/kbar (see above) and the valence-band (conduction-band) offset is larger than 200 meV (300 meV),^{7,8,23} the pressure dependence of the confinement energies can be ignored. The hydrostatic-pressure dependence of the valence-band offset is obtained from

TABLE I. Material parameters of InP, $\text{In}_{0.52}\text{Al}_{0.48}\text{As}$, InAs, AlAs, and GaAs.

	B_0^a (kbar)	B_1^a	a_0^b (Å)	c_{11}^b (kbar)	c_{12}^b (kbar)	b^b (eV)	a_{hy} (eV)
InP	710	4.93	5.869				-6.35^c
$\text{In}_{0.52}\text{Al}_{0.48}\text{As}^d$	682	3.44	5.867	1032	488	-1.66	-6.7^e
InAs	600	3.60	6.058	830	450		
AlAs	770	3.26	5.660	1250	530		
GaAs	748	3.36	5.653				

^aFrom Ref. 20.^bFrom Ref. 21.^cFrom Ref. 16.^dLinear interpolation from InAs and AlAs.^eFrom Ref. 22.

$$\frac{d\Delta E_{\text{VBO}}}{dp} = \frac{d(E_g^{\text{InP}} - E^{\text{interface}})}{dp} . \quad (5)$$

As shown in Fig. 2, the full widths at half maximum of the PL peaks remain almost constant as the pressure is increased. The hydrostatic-pressure dependence of the InP band gap and the transition energy across the interface can therefore be replaced by the dependence of the corresponding PL peaks. The difference between the energies of the peaks in the PL spectra from 0 to 35 kbar is shown in Fig. 4 and the hydrostatic-pressure derivative of the valence-band offset is linearly fitted to be 0.0 ± 0.4 meV/kbar.

B. Hydrostatic deformation potential

Because the $\text{In}_{0.52}\text{Al}_{0.48}\text{As}/\text{InP}$ interface shares neither a common anion nor cation, an interface strain^{23–26} can exist due to the difference of the P-In and In-As bond lengths as shown in Fig. 5. Although an $\text{As}_x\text{P}_{1-x}$ intermixed interface is more realistic due to the P-As exchange during the growth,²⁷ theoretical calculation of the $\text{In}_{0.53}\text{Ga}_{0.47}\text{As}/\text{InP}$ interface²⁴ showed that the valence-band offset is independent of the chemical composition at the interface. In the following, we use the abrupt interface P-In-As as shown in Fig. 5 to estimate the influence of the interface strain under pressure. First-principles calculations^{23,24} have shown that the interface strain is confined in the interface layer and can be well described by the elastic theory, i.e., the InAs layer biaxially strained on InP. Since the bond length (one-fourth of the lattice constant) changes with the hydrostatic pressure, the influence of the interface strain on the pressure dependence of the $\text{In}_{0.52}\text{Al}_{0.48}\text{As}/\text{InP}$ valence-band offset needs to be considered in order to evaluate the valence-band deformation potential. The change of the valence-band offset with the interface strain ϵ_{IS} is^{11,24,26}

$$\Delta E_{\text{IS}} = s \cdot \epsilon_{\text{IS}} ,$$

$$\epsilon_{\text{IS}} = \frac{a_p^{\text{InAs}}}{a_p^{\text{InP}}} \left\{ 1 - 2 \frac{c_{12}^{\text{InAs}}}{c_{11}^{\text{InAs}}} \left(\frac{a_p^{\text{InP}}}{a_p^{\text{InAs}}} - 1 \right) \right\} - 1 , \quad (6)$$

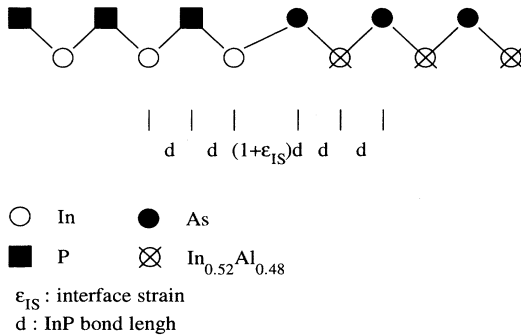


FIG. 5. Illustration of the interface strain for the $\text{In}_{0.52}\text{Al}_{0.48}\text{As}/\text{InP}$ abrupt interface.

where a_p and c_{ij} denote the lattice constant under pressure and the elastic constants as before. ϵ_{IS} is found to change from 0.067 to 0.061 in the pressure range 0 to 35 kbar. The slope s was calculated to be 1.95 eV for the $\text{In}_{0.53}\text{Ga}_{0.47}\text{As}/\text{InP}$ abrupt interface.²⁴ Since the abrupt interface configurations of $\text{In}_{0.53}\text{Ga}_{0.47}\text{As}/\text{InP}$ and $\text{In}_{0.52}\text{Al}_{0.48}\text{As}/\text{InP}$ are similar, we use the same value for the $\text{In}_{0.52}\text{Al}_{0.48}\text{As}/\text{InP}$ abrupt interface. s is estimated to be 1.9 ± 0.2 eV for the $\text{In}_{0.52}\text{Al}_{0.48}\text{As}/\text{InP}$ abrupt interface, allowing a 10% uncertainty²⁸ from the change of the InP lattice constant under pressure. The influence of the interface strain on the pressure dependence of the $\text{In}_{0.52}\text{Al}_{0.48}\text{As}/\text{InP}$ valence-band offset is determined to be -0.3 ± 0.1 meV/kbar.

The shift of the valence-band edge under hydrostatic pressure¹⁶ is

$$\Delta E_{V,p} = 3a_v \frac{\Delta a}{a_0} , \quad (7)$$

where a_v , a_0 , and Δa are the valence-band hydrostatic deformation potential, the lattice constant at zero pressure, and the pressure-induced change of the lattice constant, which is determined from the Murnaghan equation. Therefore, the valence-band hydrostatic deformation potential of $\text{In}_{0.52}\text{Al}_{0.48}\text{As}$ is obtained from the pressure dependence of the bulk valence band $\Delta E_{V,p}$, $\text{In}_{0.52}\text{Al}_{0.48}\text{As}/\text{InP}$ valence-band offset ΔE_{VBO} , and the influence of the interface strain ΔE_{IS} ,

$$\frac{d\Delta E_{\text{VBO}}}{dp} = \frac{d}{dp} (\Delta E_{V,p}^{\text{InAlAs}} - \Delta E_{V,p}^{\text{InP}} + \Delta E_{\text{IS}}) . \quad (8)$$

a_v is determined to be -0.8 ± 0.4 eV for $\text{In}_{0.52}\text{Al}_{0.48}\text{As}$, using the material parameters in Table I and the InP valence-band hydrostatic deformation potential (-0.6 eV).³

The pressure dependence of the GaAs/AlAs valence-band offset has been reported as 1.1 meV/kbar.¹² Since the GaAs/AlAs interface shares the common As atom, there is no interface strain. a_v is found to be 0.2 eV for AlAs, using the material parameters in Table I and the GaAs valence-band hydrostatic deformation potential (-0.7 eV).³ The valence-band hydrostatic deformation potentials of $\text{In}_x\text{Al}_{1-x}\text{As}$ ($0 \leq x \leq 0.52$) are linearly interpolated as $-1.9x + 0.2$ eV from those of AlAs and $\text{In}_{0.52}\text{Al}_{0.48}\text{As}$.

C. Comparison with band offset models

Two band offset models, dielectric midgap² and model-solid¹¹ theories, have been developed to predict the band-edge hydrostatic deformation potentials and the pressure dependence of the band offset. The dielectric midgap theory determines the band offset by lining up a bulk level similar to Tersoff's charge-neutrality level.²⁹ The model-solid theory puts the band positions on an absolute energy scale by modeling the solid as a superposition of neutral atoms to define an absolute average electrostatic potential within the solid. As shown in Table II,

TABLE II. Valence-band and band-gap hydrostatic deformation potentials of InP and $\text{In}_{0.52}\text{Al}_{0.48}\text{As}$ calculated from the dielectric midgap and model-solid theories.

	Dielectric midgap theory		Model-solid theory		Experiment
	a_v (eV)	a_{hy} (eV)	a_v (eV)	a_{hy} (eV)	
InP	-0.4	-5.5	1.27	-6.31	-0.6 ^a
$\text{In}_{0.52}\text{Al}_{0.48}\text{As}^b$	-0.9		1.71	-7.05	-0.8 ^c

^aFrom Ref. 3.

^bLinear interpolation from InAs and AlAs.

^cPresent study.

the calculated valence-band hydrostatic deformation potentials of InP and $\text{In}_{0.52}\text{Al}_{0.48}\text{As}$ from the dielectric midgap theory agree better with the experiments than do those from the model-solid theory. It is interesting to note that the band-gap hydrostatic deformation potentials calculated from the model-solid theory are in better agreement with the measured values than are the band-edge ones (see Tables I and II). This indicates that the model-solid theory predicts well the difference between the band-edge hydrostatic deformation potentials, but not the individual ones. The pressure dependence of the valence-band offset predicted from models is simply the difference of the pressure-induced shifts of the two bulk valence-band edges.³⁰ The pressure-induced shift of the valence-band edge is given in Eq. (7). The hydrostatic-pressure dependence of the $\text{In}_{0.52}\text{Al}_{0.48}\text{As}/\text{InP}$ valence-band offset is calculated to be 0.7 and -0.7 meV/kbar for dielectric midgap and model-solid theories respectively. These predicted pressure dependences are plotted in Fig. 4. In order to compare with the experiment, the values are uniformly shifted up 0.158 eV to match the difference between the energies of the peaks in the PL spectrum at atmospheric pressure.

The hydrostatic-pressure dependence of the valence-

band offset of some other heterostructures have also been reported. Similar to our result, the values of GaAs/AlAs,¹² GaAs/InP,³¹ and $\text{Cd}_{0.395}\text{Zn}_{0.605}\text{Te}/\text{ZnTe}$ (Ref. 32) are about 1 meV/kbar or less and compare well with the dielectric midgap and model-solid theories. Since it was indicated^{2,11} that the calculated valence-band hydrostatic deformation potentials are small and similar in magnitude to one another, this could account for the observed weak dependence of valence-band offsets under pressure. However, the pressure dependence of the InAs/GaSb valence-band offset, where the conduction-band edge of InAs is at a lower energy than the valence-band edge of GaSb, has been measured to be about 4 meV/kbar (Refs. 33, 34) and deviates from predicted values more than 2 meV/kbar.^{2,11}

IV. CONCLUSION

The hydrostatic-pressure dependence of the $\text{In}_{0.52}\text{Al}_{0.48}\text{As}/\text{InP}$ valence-band offset has been measured using PL at room temperature. The valence-band offset remains almost unchanged from 0 to 35 kbar, a range in which the lattice constant of $\text{In}_{0.52}\text{Al}_{0.48}\text{As}$ is changed by 1.5%. The pressure dependence is in good agreement with the dielectric midgap and model-solid theories. The valence-band hydrostatic deformation potential of $\text{In}_{0.52}\text{Al}_{0.48}\text{As}$ is found to be -0.8 ± 0.4 eV, which agrees well with the value calculated from the dielectric midgap theory. Using the pressure dependence of the GaAs/AlAs valence-band offset, the valence-band hydrostatic deformation potentials of $\text{In}_x\text{Al}_{1-x}\text{As}$ ($0 \leq x \leq 0.52$) are linearly interpolated as $-1.9x + 0.2$ eV.

ACKNOWLEDGMENTS

The authors would like to thank J. C. Chervin for providing the ruby spheres used in the pressure measurements. This work was supported by the NSF under the Grant No. DMR-9224877.

- ¹L. Aina, M. Mattingly, M. Burgess, R. Potter, and J. M. O'Connor, *Appl. Phys. Lett.* **59**, 1485 (1991).
²Manuel Cardona and Niels E. Christensen, *Phys. Rev. B* **35**, 6182 (1987).
³D. D. Nolte, W. Walukiewicz, and E. E. Haller, *Phys. Rev. Lett.* **59**, 501 (1987).
⁴J. M. Langer and H. Heinrich, *Phys. Rev. Lett.* **55**, 1414 (1985).
⁵E. E. Mendez, P. J. Price, and M. Heiblum, *Appl. Phys. Lett.* **45**, 294 (1984).
⁶W. Walukiewicz, H. E. Ruda, J. Lagowski, and H. C. Gatos, *Phys. Rev. B* **30**, 4571 (1984).
⁷E. J. Caine, S. Subbanna, H. Kroemer, J. L. Merz, and A. Y. Cho, *Appl. Phys. Lett.* **45**, 1123 (1984).
⁸M. J. S. P. Brasil, R. E. Nahory, W. E. Quinn, M. C. Tamargo, R. Bhat, and M. A. Koza, in *GaAs and Related Compounds 1991*, IOP Conf. Proc. No. 120 (IOP, London, 1992), p. 73.

- ⁹J. Böhrer, A. Krost, T. Wolf, and D. Bimberg, *Phys. Rev. B* **47**, 6439 (1993).
¹⁰Recently, it was suggested that the 1.2-eV luminescence arises from a transition in a thin InAs quantum well at the interface [D. Vignaud *et al.*, *J. Appl. Phys.* **76**, 2324 (1994)]. The work published in Refs. 8 and 27 has shown that a thin InAsP layer can be formed at the interface if a longer growth-halt time (> 2 s) is used by the insertion of a thin AlP layer prior to the growth halt to prevent the formation of an InAs interfacial quantum well indicates that the 1.2-eV luminescence cannot be due to such a structure.
¹¹Chris G. Van de Walle, *Phys. Rev. B* **39**, 1871 (1989).
¹²J. D. Lambkin, A. R. Adams, D. J. Dunstan, P. Dawson, and C. T. Foxon, *Phys. Rev. B* **39**, 5546 (1989).
¹³R. Bhat, M. A. Koza, K. Kash, S. J. Allen, W. P. Hong, S. A. Schwarz, G. K. Chang, and P. Lin, *J. Cryst. Growth* **108**, 441 (1991).

- ¹⁴H. K. Mao, P. M. Bell, J. W. Shamer, and D. J. Steinberg, *J. Appl. Phys.* **45**, 741 (1974).
- ¹⁵D. Ortel, D. Bimberg, R. K. Bauer, and K. W. Carey, *Appl. Phys. Lett.* **55**, 140 (1989).
- ¹⁶H. Müller, R. Trommer, M. Cardona, and P. Vogl, *Phys. Rev. B* **21**, 4879 (1980).
- ¹⁷M. Leroux, *High Pressure Res.* **1**, 149 (1989).
- ¹⁸M. Bugajski and W. Lewandowski, *J. Appl. Phys.* **57**, 521 (1985).
- ¹⁹R. People, A. Jayaraman, K. W. Wecht, D. L. Sivco, and A. Y. Cho, *Appl. Phys. Lett.* **52**, 2124 (1988).
- ²⁰B. Zhang and Marvin L. Cohen, *Phys. Rev. B* **35**, 7604 (1987).
- ²¹M. P. C. M. Krijn, *Semicond. Sci. Technol.* **6**, 27 (1991).
- ²²I. T. Ferguson, T. P. Beales, T. S. Cheng, C. M. Sotomayor-Torres, and E. G. Scott, *Semicond. Sci. Technol.* **4**, 243 (1989).
- ²³Mark S. Hybertsen, *Appl. Phys. Lett.* **58**, 1759 (1991).
- ²⁴Mark S. Hybertsen, *J. Vac. Sci. Technol. B* **8**, 773 (1990).
- ²⁵R. G. Dandrea and C. B. Duke, *J. Vac. Sci. Technol. B* **10**, 1774 (1992).
- ²⁶J. S. Nelson, S. R. Kurtz, L. R. Dawson, and J. A. Lott, *Appl. Phys. Lett.* **57**, 578 (1990).
- ²⁷M. J. S. P. Brasil, R. E. Nahory, W. E. Quinn, M. C. Tamargo, and H. H. Farrell, *Appl. Phys. Lett.* **60**, 1981 (1992).
- ²⁸Generally, s also depends on the substrate lattice constant. It was calculated in Ref. 26 that s is changed by 6% with a 2.3% uncertainty of the InAs lattice constant for the $\text{InAs}/\text{Al}_{0.8}\text{Ga}_{0.2}\text{As}_{0.14}\text{Sb}_{0.86}$ interface. In present study, the InP lattice constant has changed 1.5% in the pressure range 0–35 kbar.
- ²⁹J. Tersoff, *Phys. Rev. Lett.* **56**, 2755 (1986).
- ³⁰A pressure-induced shift of the dielectric midgap level is also included for the dielectric midgap theory, as indicated in Ref. 2.
- ³¹M. Gerling, M. E. Pistol, and L. Samuelson, *Appl. Phys. Lett.* **59**, 806 (1991).
- ³²K. Pelhos, S. A. Lee, Y. Rajakarunanayake, and J. L. Reno, *Phys. Rev. B* **51**, 13 256 (1995).
- ³³L. M. Claessen, J. C. Maan, M. Altarelli, P. Wyder, L. L. Chang, and L. Esaki, *Phys. Rev. Lett.* **57**, 2556 (1986).
- ³⁴J. Beerens, G. Gregoris, J. C. Portal, E. E. Mendez, L. L. Chang, and L. Esaki, *Phys. Rev. B* **36**, 4742 (1987).